Egypt. J. Phys. **Vol. 51,** pp. 115-134 (2023)

Egyptian Journal of Physics

https://ejphysics.journals.ekb.eg/

Case study of the Geomagnetically Induced Currents (GICs) along a hypothetical overhead Aluminum Conductor Steel Reinforced (ACSR) during active geomagnetic storms in Egypt

Nouran M. Omar[1], Tarek Arafa-Hamed[2], Mohamed Youssef Kandoul[1], Ayman Mahrous[3]

[1] *Department of physics, faculty of science, Helwan University, Cairo, Egypt.*

[2] *Department of geomagnetism, the National Research Institute of Astronomy and Geophysics (NRIAG), Cairo, Egypt.*

[3] *Basic and applied science department, faculty of engineering, Egypt-Japan University of science and technology, Alexandria, Egypt.*

SO MANY studies are made on Geomagnetically Induced Currents (GICs) around the world. Most of these studies are made in polar and equatorial latitudes due to the high intensity of GICs observed there, which are enhanced by the auroral and equatorial electrojet currents during geomagnetic storms. In this study we are going to perform our analysis at the lower latitude specifically in Egypt at periods of maximum activity of solar cycle 24. Using magnetic field data from Misallat geomagnetic station we studied the variations in the magnetic field H component in Misallat (MLT) and compared them with other stations in lower latitudes upon data availability. In most of the studied storms the maximum ($\frac{dH}{dt}$) values coincide with the Storm Sudden Commencement (SSC), while some storms have their maximum ($\frac{dH}{dt}$) during the main phase of the storm. The maximum ($\frac{dH}{dt}$) at MLT among the whole studied period is found to be 59.4 nT/min on June 22nd,2015. Finally, GIC values are estimated along the ACSR conductors with their varying resistance values showing a maximum value of 423.6 (A.Km) along the 0.0949 (Ω/km) conductor and 21.4 (A.Km) along the 1.8769 (Ω/km) conductor.

Keywords: Coronal Mass Ejection (CME), Storm Sudden Commencement (SSC), Geomagnetic Storm (GMS), geomagnetic disturbance (GMD).

Introduction

During periods of high solar activity, the sun ejects coronal mass ejections (CMEs). Some of these ejections are directed towards the Earth. When a CME hits the Earth's magnetic field, the CME's own magnetic field interacts with the Earth's magnetic field causing reconnections to occur in the magnetosphere. During this interaction the magnetosphere vibrates intensely. As a result, electric fields are induced in the ionosphere, and they could reach the Earth's surface. Consequently, induced electric field on the Earth gives rise to electric currents to flow along any conductor on the surface of the Earth. These induced electric currents are usually referred to as geomagnetically induced currents (GICs). GICs could reach tens of amperes with a maximum magnitude of about 300 A [1], its frequency is very low (varies between 0.01 Hz to 0.05 Hz), and it could last for one to three minutes [2].

GICs could be generated in any conductor on the Earth including gas pipelines, railways, and power networks that transmit electric power all over countries. GICs effect on these structures could be crucial, with the most serious effects on power plants (due to our daily reliance on electric power). Electrical components of power networks require stable voltage rates to be maintained. However, during geomagnetic storms geomagnetically induced electric fields can cause powerlines to have high voltage levels, resulting in a complete failure of some power network components. In power networks, conductors of transformer winding are highly susceptible to these faults, which may have damaging consequences on the transformer. Statistically, transformer winding failures are the most common cause of transformer faults [3].

On 13th March 1989, a CME hits the Earth causing serious damage to the Hydro Quebec power network. This is due to GIC generation through the power network that leads to a cutoff from the major generation source, which leads to a total black out that lasts for about 9 hours [4]. Another accident on 24th March 1991, on this day GICs caused damages to the Radisson-Sandy Pond high voltage direct current (HVDC) link. About a 110 A were

*Corresponding author: Nouran M. Omar, E-mail: noranomar32@gmail.com, Tel.: +2 01288966587
Received: 15/08/2023; Accepted: 30/09/2023
DOI: 10.21608/EJPHYSICS.2023.227683.1091

measured at one of two parallel transformers at substation of Radisson (totally about 220 A), this amount of GIC led to a loss of the high voltage direct current (HVDC) link [4]. These two accidents costed Canada enormous amounts of money. So, to be able to mitigate such destructive effects, GICs should be studied well and power system characteristics should be taken into consideration as well.

GIC threats power networks all over the world. Indeed, it has been found that GICs have considerable impact on power plants at high latitudes because of auroral electrojet current. However, at times of geomagnetic storms GICs impact could extend to mid and low latitudes [4,7,6]. [8] In his study of GIC measured at two equatorial stations found that the intensity of GIC is doubled at the equator than it is a few degrees to the north. This means that there is a GIC enhancement at the equator and the reason is the equatorial electrojet current (EEJ), which is consistent with other studies [9, 10, 11]. Figure 1 shows the change of the average maximum of dB/dt over latitude. It is obvious that dB/dt has its maximum value at the magnetic dip equator, while stations outside the equatorial region ($\sim \pm 15°$) have less dB/dt levels [12]. Consequently, stations near the magnetic equator are more susceptible to higher GIC risk levels than stations at low latitudes.

In fact, the occurrence of GICs does not only depend on the latitude of the region but it also depends on the

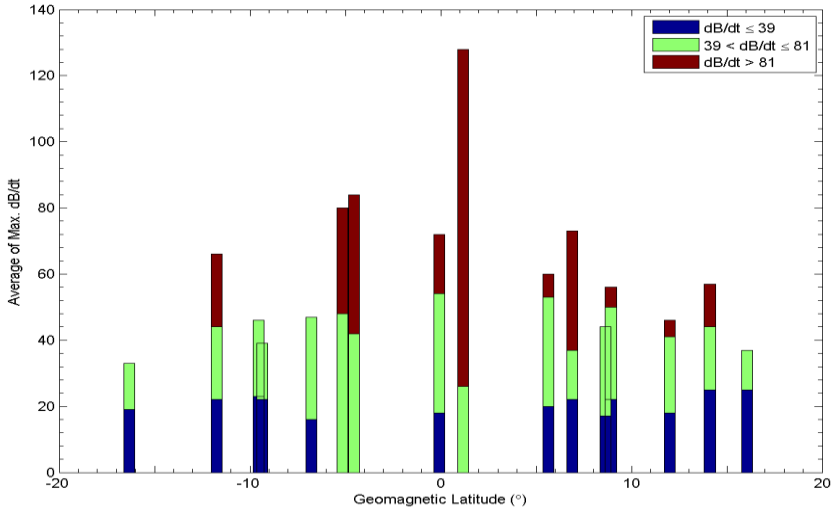

Fig. 1. represents the average of max. dB/dt at latitudinal range from the dip equator at 0° to low latitude at 20°north and south. dB/dt is classified at low, medium and high in blue, green, and red respectively. From [12]

power network characteristics. Direction of the power line, length of powerline and resistance of the power system conductors are the most important characteristics to be taken into consideration. Magnitudes of GIC in a power line depend on the direction of geomagnetically induced electric field (GIE) with respect to the direction of the power line, and the maximum GIC values occur when GIE direction is parallel to the power line direction [13].

Studies showed that GICs relay on the length of the power system, and they can be calculated by dividing the electric field by the resistance of the line per unit length [13]. Line length has been studied as a GIC risk factor in multiple research projects. However, if the line is part of a broader network that permits GIC to continue flowing from one transmission line to the next one, GIC would not need to flow to or from the ground at the ends of the long line. Instead, GIC flow to/from the ground through substations located at the edge of a network. This is called "the edge effect".

One of the important indicators on GIC occurrence is the rate of change of the magnetic field with time ($\frac{dB}{dt}$). According to maxwell faraday's law of induction (equation 3); any variation in the magnetic field leads to an induction of electric field. Multiple studies of GIC are made Based on Maxwell- Faraday's law of induction [5, 9, 10, 14]. It is found that the magnetic horizontal component (H) is the most relevant component to predict GIC occurrence; therefore, calculating the rate of change of the magnetic H component with time ($\frac{dH}{dt}$) is a good indicator for GIC occurrence. In order to predict a probable GIC occurrence, the rate of change of magnetic field with time have to exceed 30 nT/min [5, 14].

In this study we investigate GICs through the rate of change of the magnetic field H component (dH/dt) during the maximum activity of solar cycle 24, from 2012 to 2017, in Egypt. Our data are collected from Misallat

geomagnetic station in Egypt, to investigate GICs in Egypt. MLT station is chosen due to its location in Egypt, which is a mid-latitude region. Additionally, we compared our results with results obtained from equatorial stations, which are, Langkawi (LKW), Bac Lieu (BCL), Pontianak (PTN), their coordinates are listed in table 1. Comparisons are made between MLT station and other equatorial stations to compose clear insights about low and equatorial latitude regions. We applied our calculations on the ACSR conductor as it is approved by the Egyptian electricity holding company, and its specifications could be found on "https://www.eehc.gov.eg/CMSEehc/media/53slvg1m/edms-04-100-1.pdf" (page 7). Finally, we estimated GIC values along a hypothetical overhead ACSR conductor during the studied storms. The maximum and minimum calculated GIC values along the ACSR conductor with the lowest resistance 0.0949 (Ω/km) are 423.6 (A.Km) and 315 (A.Km) respectively. On the other hand, the maximum and minimum calculated GIC values along the ACSR conductor with the highest resistance 1.8769 (Ω/km) are 21.4 (A.Km) and 15.9 (A.Km) respectively.

Although GICs investigations have been conducted in different countries around the world, it is the first time to conduct real calculations of GICs over Egypt, besides applying calculations on the ACSR conductor. This study is made to better understand the severity of GICs over Egyptian powerlines, to find out if GICs have a real threat over Egypt. We figured Egypt is frequently susceptible to GICs during strong geomagnetic storms.

Experimental

The aim of this research is to study the severity of GICs in Egypt using the time derivative of the geomagnetic field horizontal component (dH/dt). The geomagnetic filed data are collected from Misallat station upon data availability. The maximum (dH/dt) value for each studied day is then manipulated in table 2 and compared against [5] results, which are calculated at equatorial stations (BCL, LKW, PTN). Full names and geomagnetic coordinates for each station are tabulated in table 1. After obtaining the maximum (dH/dt) from MLT station we estimated the maximum GICs generated along the ACSR conductors using the maximum dH/dt and their different resistance values. In order to establish our goal, the following steps have been taken.

i- Days of high geomagnetic activity to be studied are selected depending on the kp index value which indicates the geomagnetic activity of the day. Kp index spans values from 1 to 9. From 1 to 4 indicates low activity levels, from 5 to 7 minor storm levels, while higher than 7 is a severe storm (https://kp.gfz-potsdam.de/en/). The selected days of our study are chosen to be the most active days of solar cycle 24 (2012-2017).

ii- We have collected geomagnetic field data from ground magnetometer located at the Misallat (MLT) geomagnetic station upon data availability with geomagnetic coordinates of 26.81 N and 108.30 E. Our magnetometer records magnetic field data every one second. So, the data is downsampled into one minute sampling rate.

iii- Besides, Symmetric disturbance field in H (SYMH) index and AU&AL indices are downloaded from the World Data Center (WDC) for Geomagnetism, Kyoto website (https://wdc.kugi.kyoto-u.ac.jp/wdc/Sec3.html). The purpose of the AU and AL indices is to represent, respectively, the largest current strength of the eastward and westward auroral electrojets according to the National Oceanic and Atmospheric Administration (NOAA). SYMH-index provides the geomagnetic storm's typical magnetic signature, as it provides the geomagnetic storm diverse phases (initial phase, main phase and recovery phase).

iv- Previous studies have shown that there is a strong correlation between GIC and the time derivative of the horizontal component (dH/dt). As a result, dH/dt can be utilized as a reliable indicator of GIC occurrence on Earth's surface with a lower threshold of 30 nT/min [5, 14]. So, in order to estimate the probability of GIC occurrence the time derivative of the geomagnetic field horizontal component (dH/dt) is calculated using Eq. 1 [14] and used as a proxy of the induced voltage on Earth.

$$\frac{dH}{dt} = \sqrt{\left(\frac{dx}{dt}\right)^2 + \left(\frac{dy}{dt}\right)^2} \qquad (1)$$

v- The maximum calculated dH/dt values are then manipulated to calculate GICs values along the ACSR conductors. GICs are then calculated using Ohm's law, for each different resistance for the ACSR conductors using Eq. 2 [15].

$$GIC = V/R \qquad (2)$$

Such that, V is the induced voltage and R is the resistance of the transmission line, in our case the resistance of the ACSR conductor. Characteristics of the ACSR conductor could be found on, https://www.eehc.gov.eg/CMSEehc/media/53slvg1m/edms-04-100-1.pdf, and the conductor's resistance per unit length used in this study is tabulated in table (3).

According to Maxwell- Faraday law of induction (Eq. 3) [15], the induced voltage equals the time derivative of the magnetic field (dH/dt), which is previously calculated from Eq. 1. Hence, by plugging (dH/dt) values, only, exceeding 30 nT/min for each storm day and the ACSR's resistance per unit length into Eq.2 the geomagnetically induced current along the ACSR conductor can be estimated. This step is made for each storm day, using (dH/dt) values exceeding 30 nT/min for this day and the variable resistance provided in table 3.

$$\mathbf{V} = \int E.dl = \nabla \times E = -\frac{\boldsymbol{dH}}{\boldsymbol{dt}} \qquad (3)$$

vi- Finally, the relation between the conductor's resistance and the estimated GIC is displayed and discussed.

TABLE 1. names and abbreviations for each geomagnetic station and their geomagnetic coordinates

Station Name	GM Lat.	GM Long.
Misallat, MLT	26.81	108.30
Bac Lieu, BCL	-0.36	178.36
Langkawi, LKW	-3.30	172.44
Pontianak, PTN	-9.75	181.96

Results and Discussion

In this study we inspect the geomagnetically induced currents GICs in powerlines located in Egypt during the period from 2012 to 2017. CMEs and coronal holes (CH) are responsible for driving fast solar wind towards the Earth, causing high solar wind dynamic pressure. The high solar wind pressure pushes the magnetosphere causing sharp variations in the magnetosphere which is called sudden storm commencement SSC or sudden impulse SI, each are classified according to its signature in the magnetic horizontal component (H) [11].

Here we use the rate of change of the magnetic horizontal component ($\frac{\mathrm{dH}}{\mathrm{dt}}$) [17], as a representative of the electromotive force generated in the conductor.

Our obtained results include the measured geomagnetic field horizontal component data (H), the time derivative of the magnetic H component ($\frac{dH}{dt}$), The maximum ($\frac{dH}{dt}$) value and the calculated GICs using Maxwell Faraday Equation and Ohm's law as mentioned previously in the methodology.

Firstly, we calculated the maximum ($\frac{dH}{dt}$) at the MLT station and compared its values with LKW, BCL and PTN stations within the data availability. These results are listed in table 2 with the stations' latitudes and dates of studied storms.

Year 2012:

We studied two events through 2012, the first event on 24th January and the second one on 15th July. Our data collected from Misallat station is shown in figure 3 and compared with results at the BCL, LKW, and PTN stations, their geomagnetic latitudes are mentioned in Table 2.

Data on 24th January:

On 24th January 2012 a CME hits the Earth's magnetosphere at approximately 1500 UT (1700 Misallat local time) developing a geomagnetic storm. The storm commenced at 1500 UT as obvious in SYMH and (AU, AL) indices. it was a G1-class GMS with a maximum Kp index of 5 (figure 2). The CME interaction with the magnetosphere caused sharp variations in the H component as shown in figure 3. b. which resulted in dramatic increase at the rate of change of the H component ($\frac{dH}{dt}$) in all of the four stations (MLT, BCL, LKW, and PTN). Where LKW has the maximum value of 34.83 nT/min followed by BCL, MLT and PTN in descending order. Figure 3. a. shows that both MLT and LKW have their maximum ($\frac{dH}{dt}$) values of 21 nT/min and 34.83 nT/min

respectively at the same time of the CME arrival (1500 UT). Whereas MLT and PTN have the minimum ($\frac{dH}{dt}$) values of 21 nT/min and 7.3 nT/min respectively. On figure 3. b. the magnetic field H component at MLT and LKW are almost comparable at times of abrupt variations.

Table 2. Calculated values of maximum ($\frac{dH}{dt}$) at the Misallat station compared with results from other stations taken from [5], through the period from 2012 to 2017. Table columns from left to right are, storm date- Universal time of the maximum dH/dt- local time of Misallat station- maximum dH/dt values for (LKW, BCL, PTN and MLT) stations.

Date	UT (Hr)	LT (Hr) of MLT station	MAX. dH/dt(nT/min)			
			LKW GM Lat. (-3.30)	BCL GM Lat. (-0.36)	PTN GM Lat. (-9.75)	MLT GM Lat. (26.81)
24-Jan 12	15:04	**17:04**	34.83	-22.19	7.33	**21**
15-Jul 12	6:43	**8:43**	30.3	-25.89	-10.53	**9.3**
17-Mar13	06:00	**8:00**	41.2	46.52	38.01	**40.2**
2-Oct 13	4:35	**6:35**	88.28	92.98	33.70	**33.9**
8-Feb 14	3:06	**5:06**	30.8	32.79	-	**11**
16-Feb 14	4:50	**6:50**	35.11	33.23	-	**8.8**
12-Sep 14	15:54	**17:54**	31.46	36.24	-	**36.9**
23-Dec 14	11:15	**13:15**	40.44	40.12		**47.9**

Data on 15th July:

Figure 5 shows the impact of the CME (that hit the Earth on 14th of July at about 1800UT) on the magnetic field H component the following day of the strike. On July 15th, the magnetic field continued to reverberate, developing a geomagnetic storm. It was a G1 minor storm with a maximum Kp index of 5. We can observe the impact of the storm at about 6:40 UT (8:40 Misallat local time) on both the SYMH and (AU, AL) indices (figure 4). As a result, stations at different latitudes recorded different values of ($\frac{dH}{dt}$). Where LKW recorded the largest value of 30.3 nT/min followed by BCL, PTN, and MLT. Figure 5. a. shows that MLT and PTN recorded the minimum ($\frac{dH}{dt}$) values of 9.3 nT/min and -10.53 nT/min respectively at about 6:43 UT.

Regarding the collected data in the year 2012 through two different storms, we can notice that our calculated ($\frac{dH}{dt}$) at MLT are almost comparable to those results obtained from PTN station. This may be due to the resemblance of the ionospheric nature above both stations; where both stations are located at low latitude regions

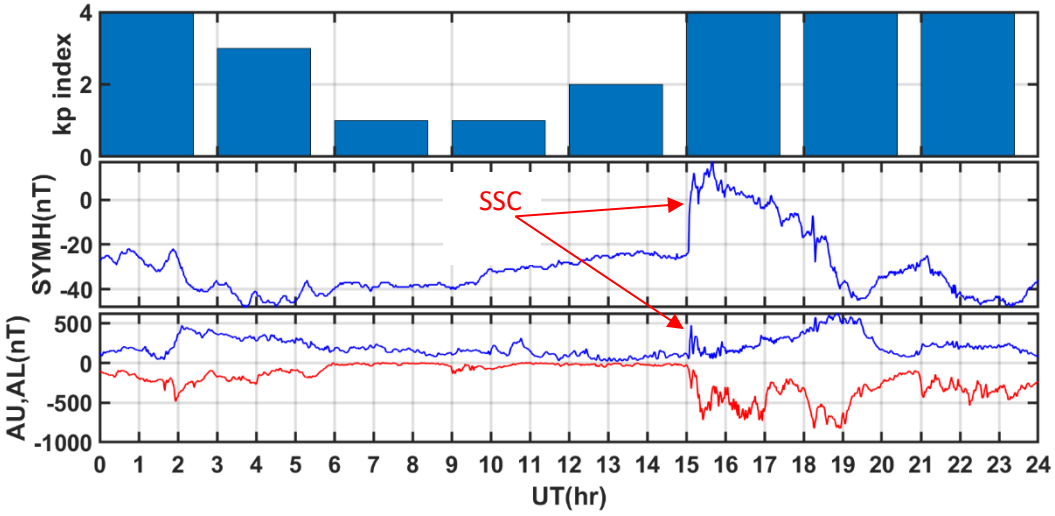

Fig. 2. Geomagnetic activity indices on January 24th , 2012. The panels from top to bottom, kp index, SYMH index in nT finally, AU (blue) and AL (red) indices in nT.

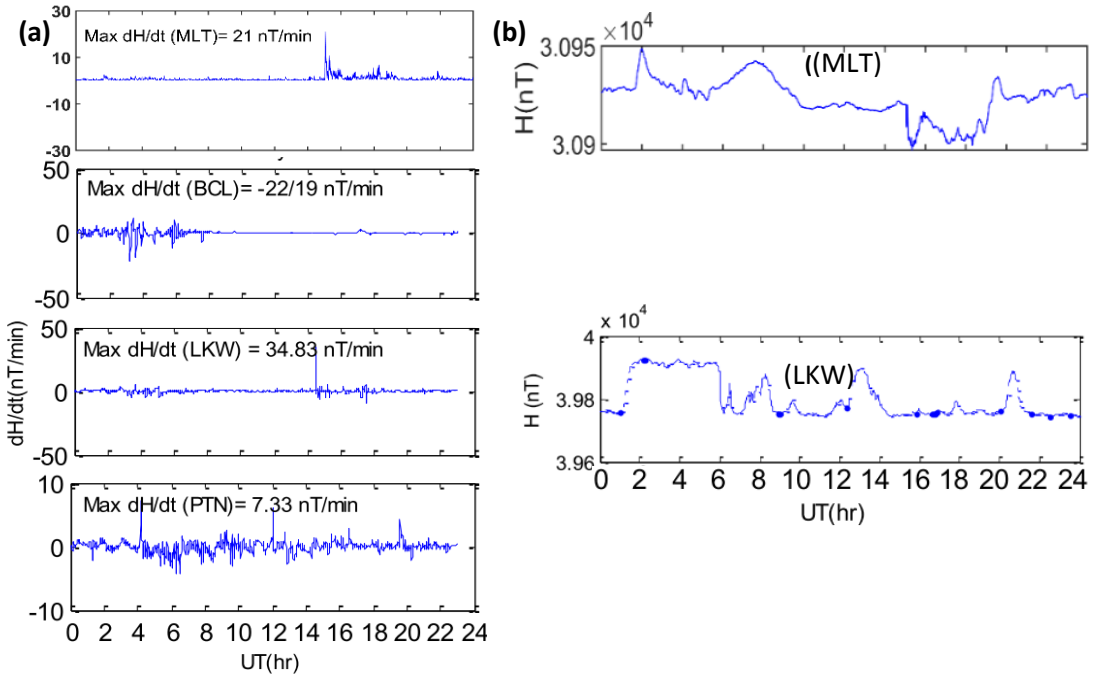

Fig. 3. (a) represents the calculated (dH/dt) values, and (b) represents the Measured magnetic field H component for the four stations MLT, BCL, LKW, and PTN from top to bottom on 24th Jan. 2012.

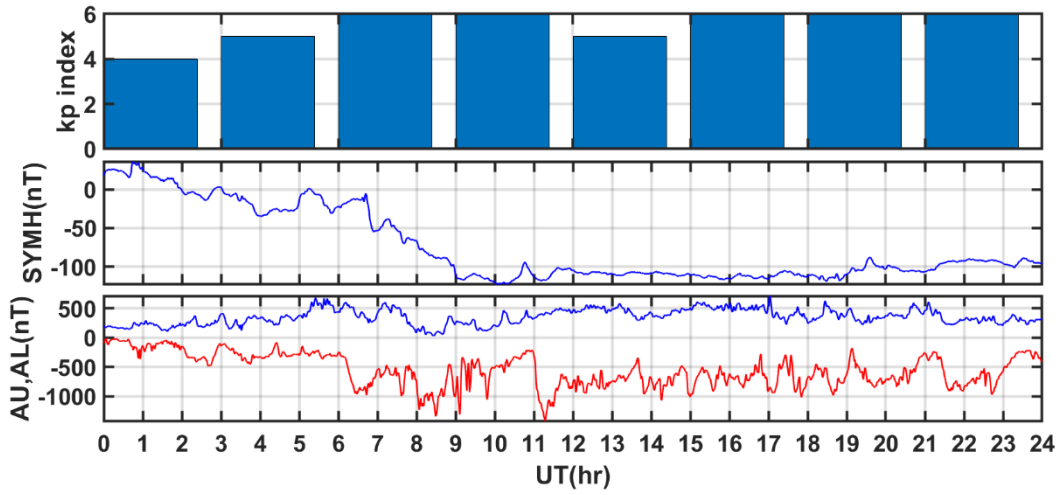

Fig. 4. Geomagnetic activity indices on July 15th , 2012. The panels from top to bottom, kp index, SYMH index in nT finally, AU (blue) and AL (red) indices in nT.

that face the same ionospheric conditions.

Year 2013

We studied two high activity events throughout the year 2013, the first event on 17th March and the second one on 2nd October.

Data on 17th March:

On March 17th, a CME struck the Earth at 06:00 UT causing a G2- class GMS with a maximum Kp index of 6. The storm commenced 06:00 UT (08:00 Misallat local time) at daytime showing this sudden variation in both SYMH and (AU, AL) indices (figure 6). As well as a sudden increase in the magnetic field H component in BCL, LKW, and PTN, while a sudden decrease in MLT station magnetic H component occurred at 08:00 local time for MLT station, as shown in figure 7. b. As a result, the time derivative of the H component ($\frac{dH}{dt}$) peaked in

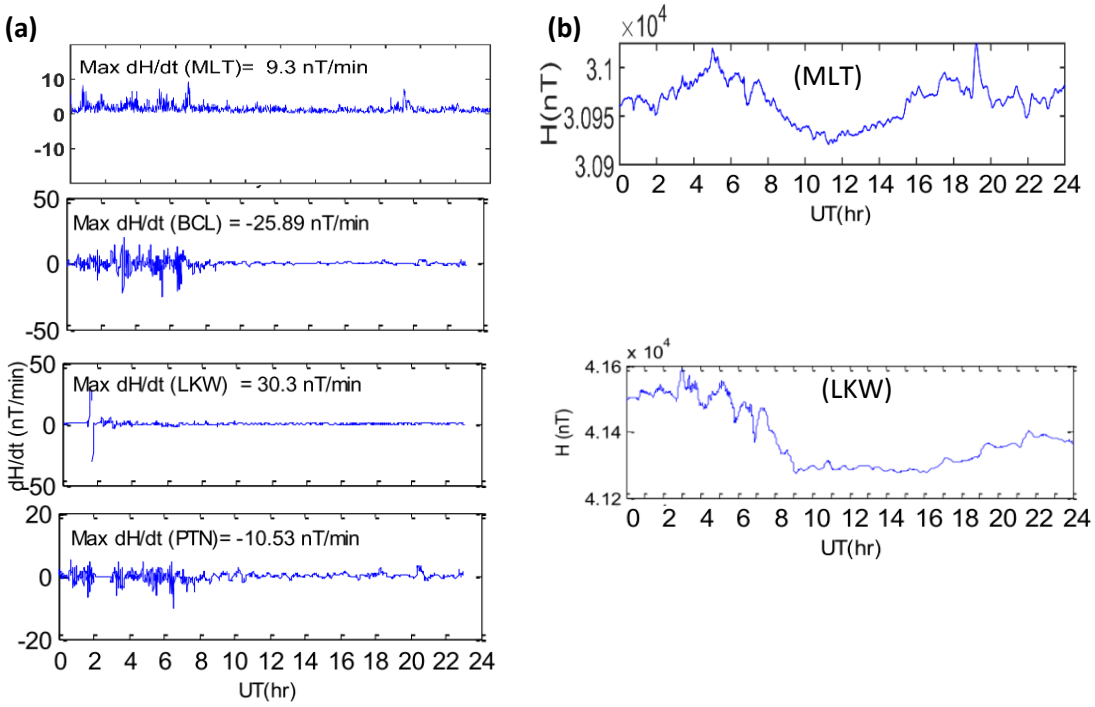

Fig. 5. (a) represents the calculated (dH/dt) values, and (b) represents the Measured magnetic field H component for the four stations MLT, BCL, LKW, and PTN from top to bottom on 15th Jul. 2012.

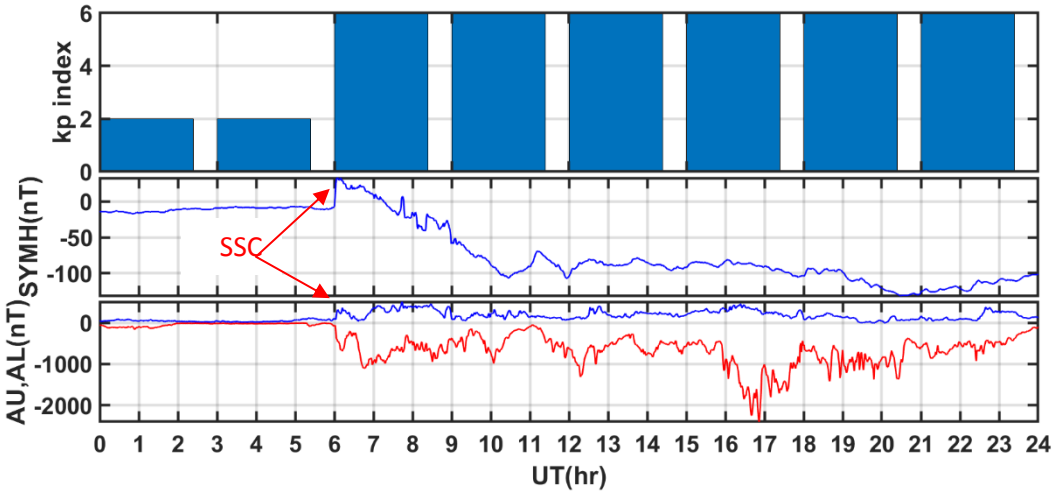

Fig. 6. Geomagnetic activity indices on March 17th , 2013. The panels from top to bottom, kp index, SYMH index in nT finally, AU (blue) and AL (red) indices in nT.

the four stations at 06:00 UT. Where ($\frac{dH}{dt}$) recorded a maximum value of 46.52 nT/min at BCL, while MLT recorded 40.2 nT/min, as shown in figure 7. a.

Data on 2nd October:

A CME hit the Earth at the early hours of 2nd October 2013 developed a geomagnetic storm of G2- class with a maximum Kp index of 6. The CME struck at about 0200 UT (0400 Misallat local time) during the daytime, causing a sudden commencement at that time. The commencement caused a sudden change in both SYMH and (AU, AL) indices at 0200 UT (figure 8). Consequently, the SSC resulted in sharp variations in the H component along the four stations as illustrated in figure 9. b. Calculated ($\frac{dH}{dt}$) recorded a maximum peak of 92.98 nT/min,

88.28 nT/min, and 33.79 nT/min in BCL, LKW, and PTN respectively at around 01:58 UT; on the other hand($\frac{dH}{dt}$) recorded a maximum value of 33.9 nT/min at MLT at 4:35 UT of the same day (figure 9. a.).

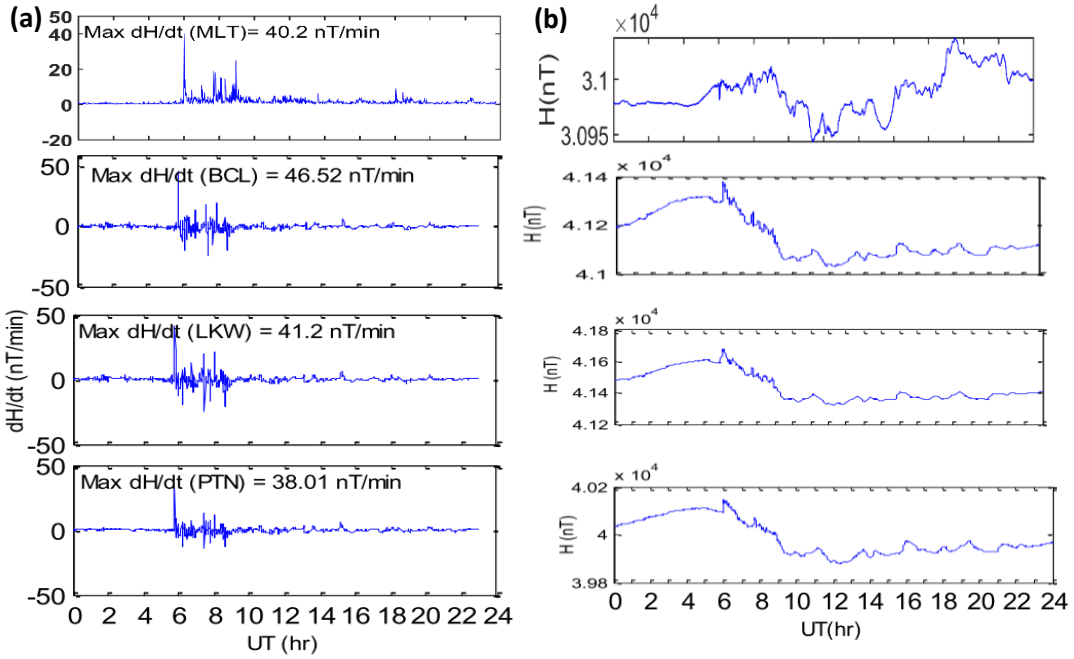

Fig. 7. (a) represents the calculated (dH/dt) values, and (b) represents the Measured magnetic field H component for the four stations MLT, BCL, LKW, and PTN from top to bottom on 17th of March 2013.

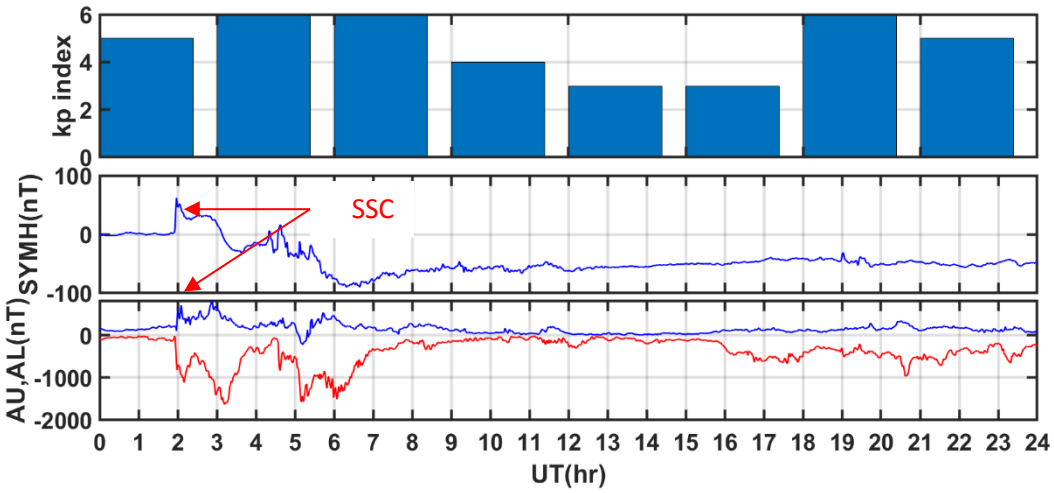

Fig. 8. Geomagnetic activity indices on October 2nd, 2013. The panels from top to bottom, kp index, SYMH index in nT finally, AU (blue) and AL (red) indices in nT.

In reviewing 2013 results, we found that, in the two events of March and April, our results from the MLT station were less than its corresponding. This may be due to its low latitude location far from the equatorial electrojet current, which highly enhances GICs at the equatorial sector.

Year 2014:

We studied four high activity events through the year 2014, the first event on 8th February, 16th February, 12th September, and 23rd December.

Data on 8th February:

A minor CME hit the Earth the previous day at nearly 17:00 UT, and a C8 X-ray solar flare that occurred on 8th February together triggered perturbations in the magnetosphere. At the early hours of the day (between 01:00 to 03:00 UT) kp index has its maximum value of 5, also SYMH and (AU, AL) had sharp variations at the same time as shown in figure 10. As a result, the magnetic field H component reverberated frequently, as shown in figure 11. b., enhancing ($\frac{dH}{dt}$) in our studied stations. Figure 11. a. represents the maximum ($\frac{dH}{dt}$) values in each station, where BCL has the highest value of 32.79 nT/min while MLT has the lowest value of 11 nT/min at approximately 03:00 UT (05:00 LT, afternoon).

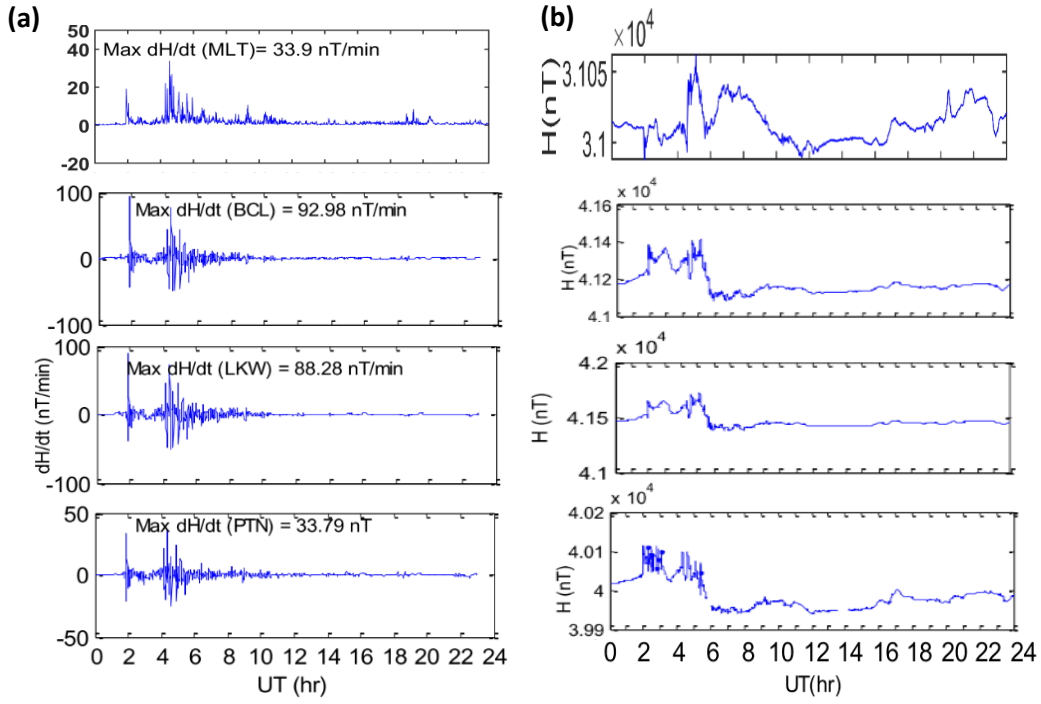

Fig. 9. (a) represents the calculated (dH/dt) values, and (b) represents the Measured magnetic field H component for the four stations MLT, BCL, LKW, and PTN from top to bottom on October 2nd, 2013.

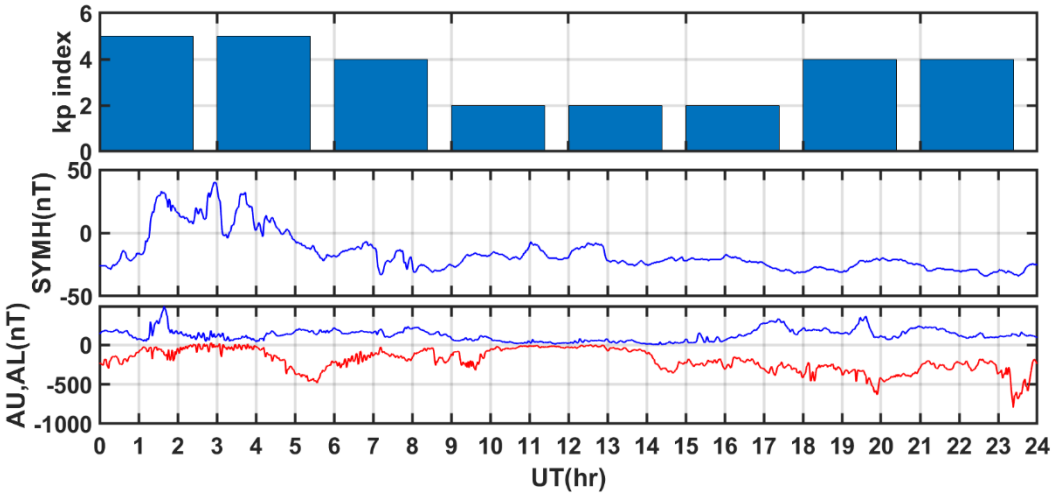

Fig. 10. Geomagnetic activity indices on February 8th, 2014. The panels from top to bottom, kp index, SYMH index in nT finally, AU (blue) and AL (red) indices in nT.

Data on 16th February:

On 15th February a cannibal CME hit the Earth's magnetic field. the impact did not develop a geomagnetic storm although the CME was a merger of three minor clouds. It just maintained an unstable magnetic field, causing moderate perturbations in the magnetic field H component as shown in figure 13. b. As a result , $(\frac{dH}{dt})$ peaked at 04:30 UT (06:30 LT) in all of the three stations, with its maximum value of 35.11 nT/min at LKW and minimum value of 8.8 nT/min at MLT (figure 13. a.). The time of the $(\frac{dH}{dt})$ peak coinsided with a sudden decrease in the

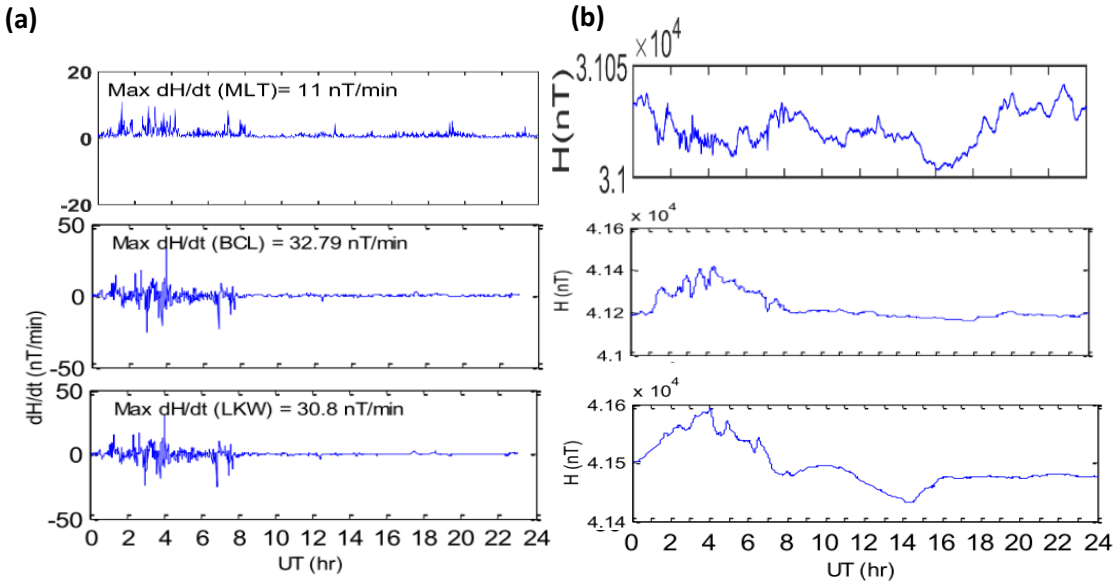

Fig. 11. (a) represents the calculated (dH/dt) values, and (b) represents the Measured magnetic field H component for the three stations MLT, BCL, and LKW from top to bottom on 8th February 2014.

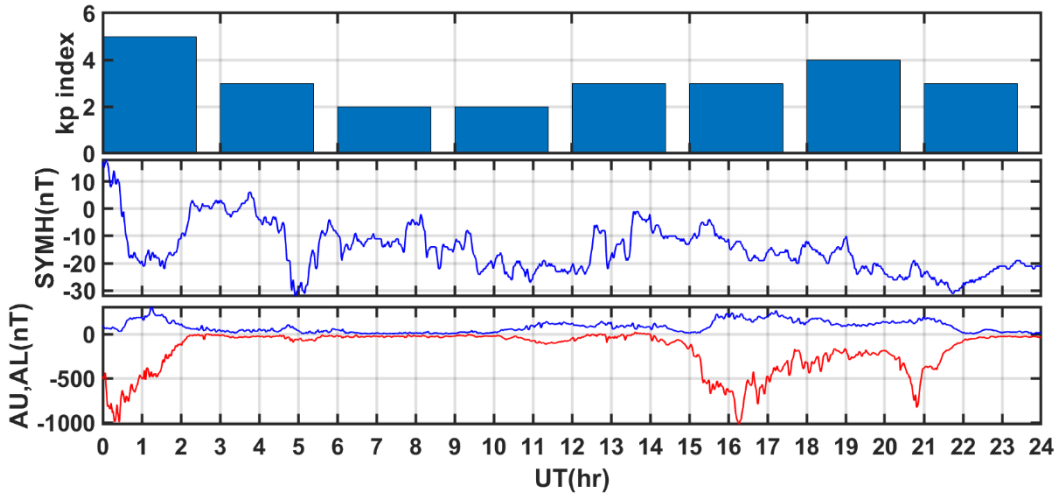

Fig. 12. Geomagnetic activity indices on February 16th, 2014. The panels from top to bottom, kp index, SYMH index in nT finally, AU (blue) and AL (red) indices in nT.

SYMH; However, Kp index has a maximum value of 5 at the first three hours of the day (figure 12).

Data on 12th September:

Two successive CMEs hit the Earth's magnetic field on 11th and 12th September causing a geomagnetic storm that has its peak on 12th September 2014. At 16:00 UT the CME hit the magnetosphere causing a G2- class GMS

with maximum KP index of 6. Also, we can observe the commencement in both SYMH and (AU, AL) at the same time as shown in figure 14. This storm resulted in large perturbations in the magnetic field H component for the three stations which exhibit a disturbance signature that is comparable among the three stations in figure

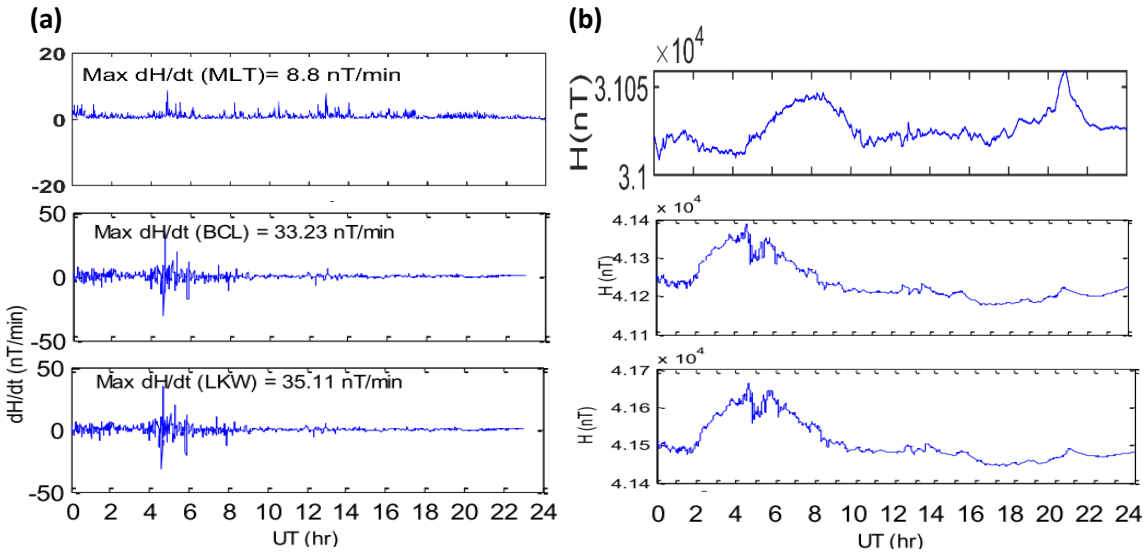

Fig. 13. (a) represents the calculated (dH/dt) values, and (b) represents the Measured magnetic field H component for the three stations MLT, BCL, and LKW from top to bottom on 16th February 2014.

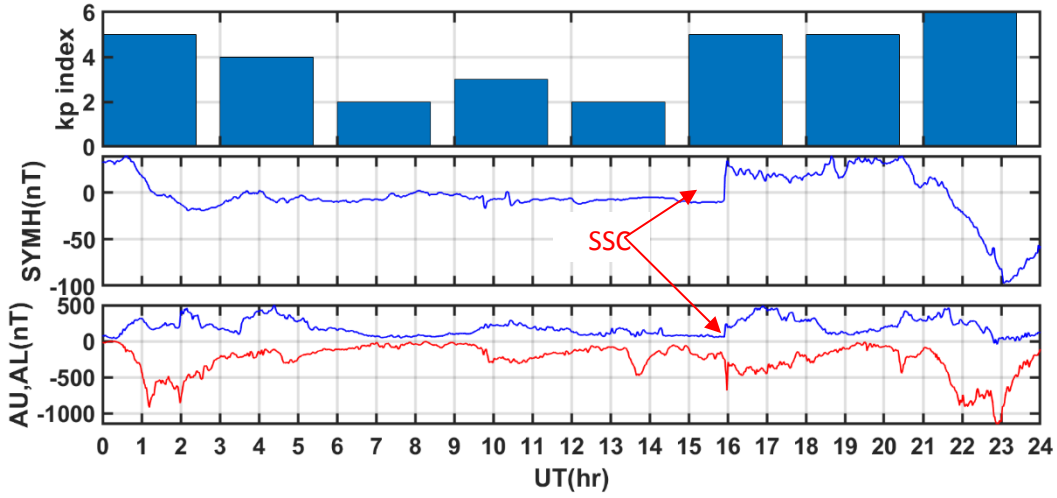

Fig. 14. Geomagnetic activity indices on September 12th, 2014. The panels from top to bottom, kp index, SYMH index in nT finally, AU (blue) and AL (red) indices in nT.

15. b. As a result, the time derivative of the H component peaks at 15:54 UT (17:54 LT, at night for MLT) for the three stations. Where, for the first time, MLT has the maximum ($\frac{dH}{dt}$) value of 36.9 nT/min followed by BCL and LKW, as shown in figure 15. a.

Data on 23rd December:

During the early hours of 23rdDecember a CME sideswiped the Earth's magnetic field resulting in an abrupt change in the magnetic field H component at nearly 11:15 UT (13:15 LT, at noon in MLT). The maximum KP index recorded was 4 at the time of the storm commencement, which is represented in both the SYMH and (AU, AL) indices (at 11:15 UT) in figure 16. Consequently, the time derivative of the H component peaked at the same time (11:15 UT), showing a maximum ($\frac{dH}{dt}$) value of 47.9 nt/min in MLT station followed by LKW and BCL (figure 17. a.).

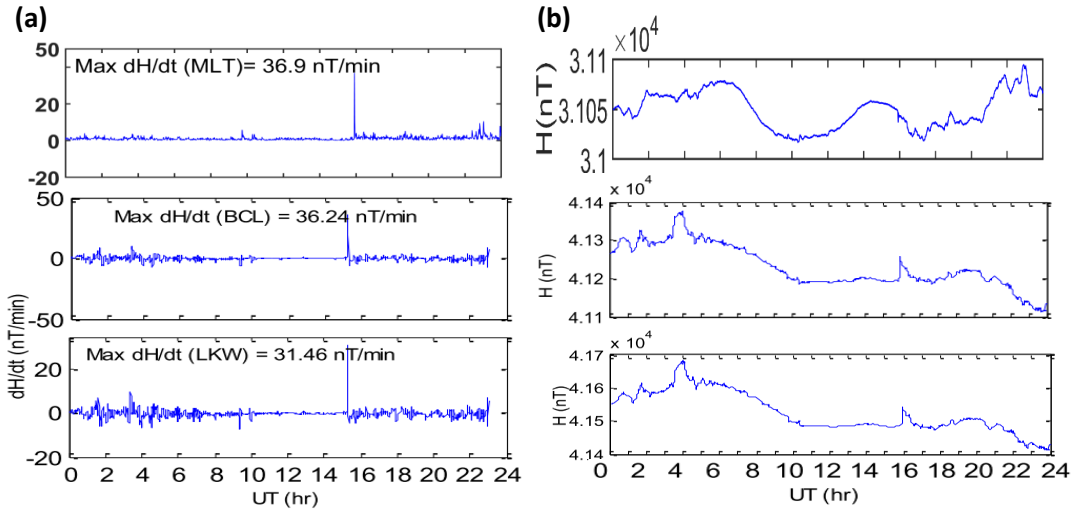

Fig. 15. (a) represents the calculated (dH/dt) values, and (b) represents the Measured magnetic field H component for the three stations MLT, BCL, and LKW from top to bottom on 12th September 2014.

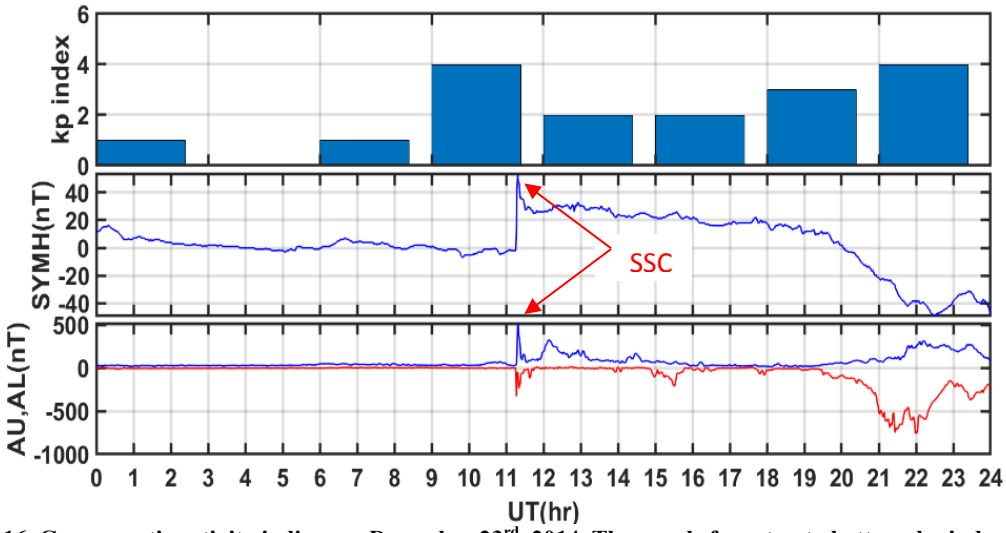

Fig. 16. Geomagnetic activity indices on December 23rd, 2014. The panels from top to bottom, kp index, SYMH index in nT finally, AU (blue) and AL (red) indices in nT.

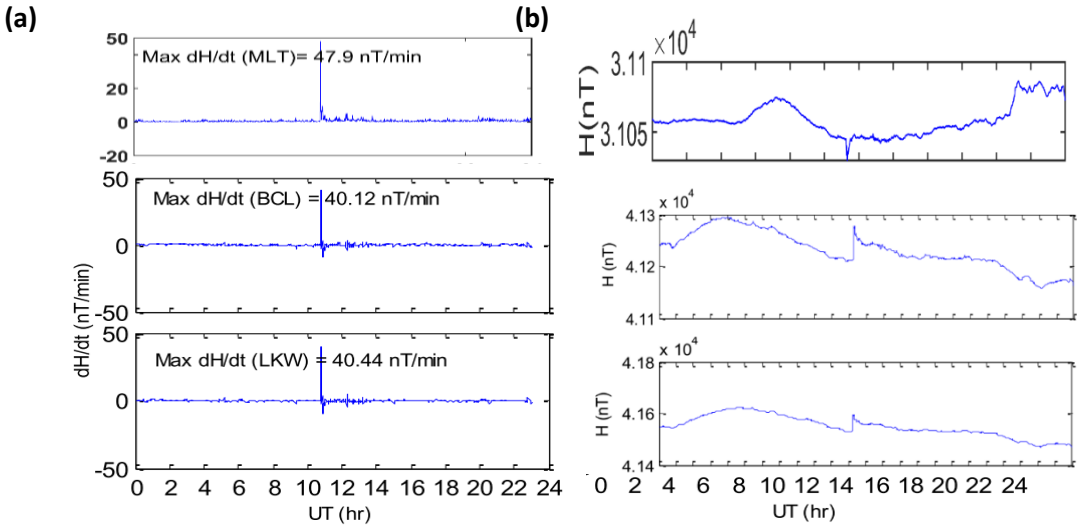

Fig. 17. (a) represents the calculated (dH/dt) values, and (b) represents the Measured magnetic field H component for the three stations MLT, BCL, and LKW from top to bottom on 23rd December 2014.

Year 2015:

2015 is considered to be the highest active year of solar cycle 24, as it has the maximum sunspot number (SSN) among solar cycle 24. We studied three high activity events through the year 2015. The first event was recorded to be on two following days 22nd and 23rd of June 2015, the second one was on 17th of March 2015.

Data on 22nd & 23rd June:

On June 22nd a series of CMEs struck the Earth's magnetic field, developing a geomagnetic storm (GMS) whose effect lasted for two days, 22nd and 23rd of June. On the first day the GMS was a severe G4-class storm with a maximum Kp index of 8, the storm commenced at 18:30 UT as represented in SYMH and AU, AL indices (figure 18). A strong M6.5 solar flare erupted releasing electrons and protons towards the Earth. The flare was detected by the Solar Dynamics Observatory of NASA at 18:23 UT. By that time, an abrupt change occurred in the magnetic field H component at about 18:30 UT. Consequently, the time derivative of the H component ($\frac{dH}{dt}$) peaked to have a maximum value of 59.4 nT/min at that time as obvious in figure 19. a. The effect of CMEs on the Earth's magnetic field extended to June 23rd, yet having a minor GMS. Perturbations continued progression in the magnetic H component causing a maximum ($\frac{dH}{dt}$) value of 16.7 nT/min at 2 UT as presented in figure 19.b.

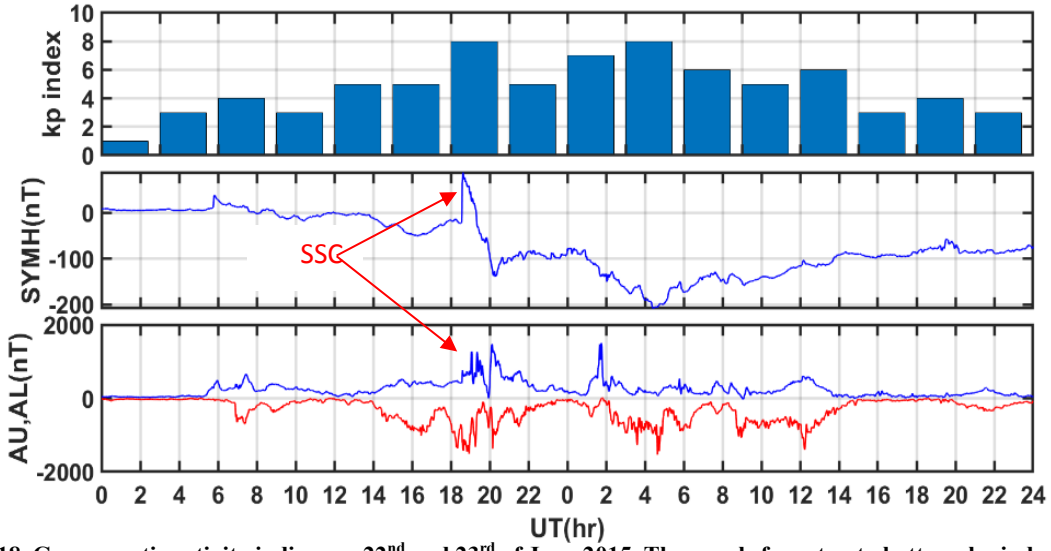

Fig. 18. Geomagnetic activity indices on 22nd and 23rd of June 2015. The panels from top to bottom, kp index, SYMH index in nT finally, AU (blue) and AL (red) indices in nT.

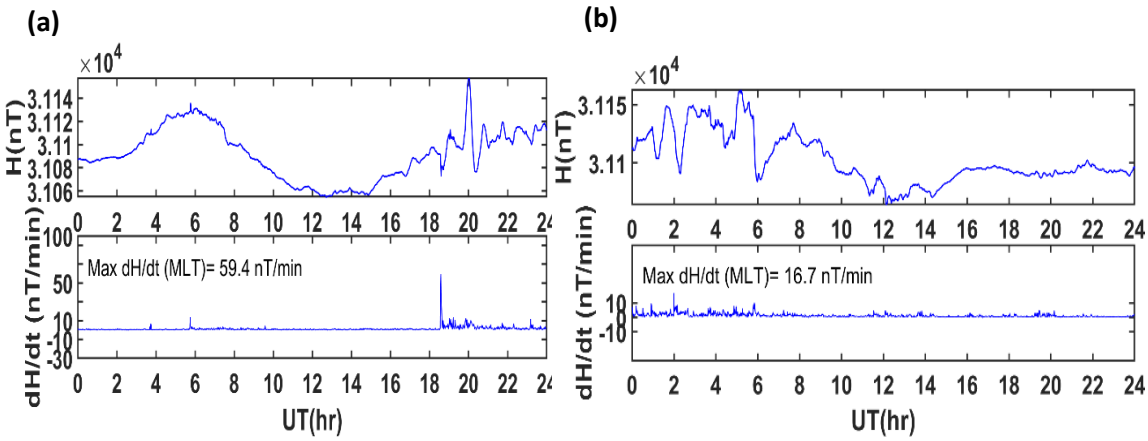

Fig. 19. (a) represents the Measured magnetic field H component and calculated (dH/dt) values for MLT station on June 22nd, 2015 and (b) represents the same variables on June 23rd 2015.

Data on 17th of March:

Saint Patrick's storm, on March 17th a CME hit the magnetosphere causing a GMS, the storm commenced at 04:48 UT as obvious at the SYMH and AU, AL indices (figure 20). At the beginning, the impact resulted in a G1- class geomagnetic storm (kp= 5). Then the storm got intensified till reaching a G4- class GMS with a maximum kp index of 8.

zThe impact of CME interaction with the magnetosphere was tremendous, as it resulted in sharp variations in the magnetic H component. Consequently, a maximum peak of 59.2 nT/min in the $(\frac{dH}{dt})$ developed at 4:48 UT (figure21), which is the highest GMS impact among all storms of solar cycle 24.

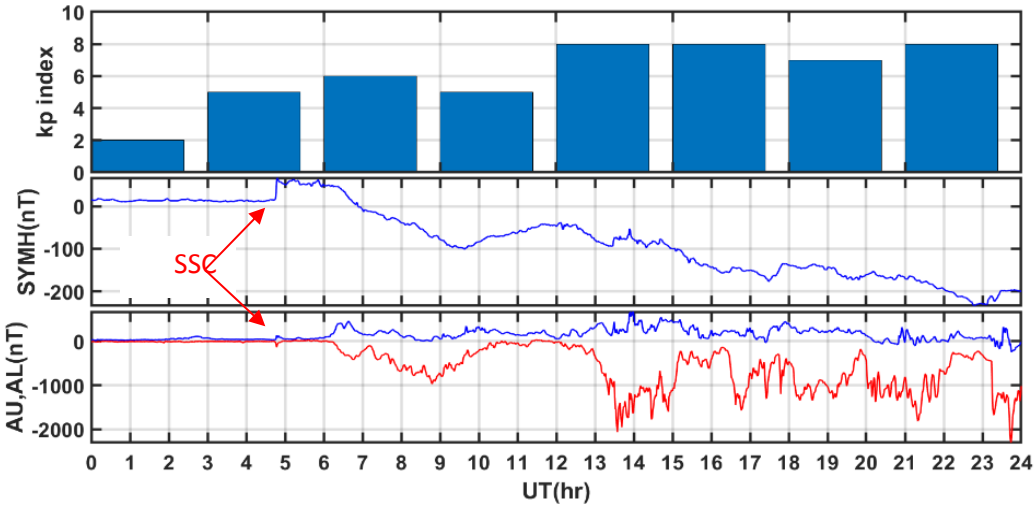

Fig. 20. Geomagnetic activity indices on March 17th, 2015. The panels from top to bottom, kp index, SYMH index in nT finally, AU (blue) and AL (red) indices in nT.

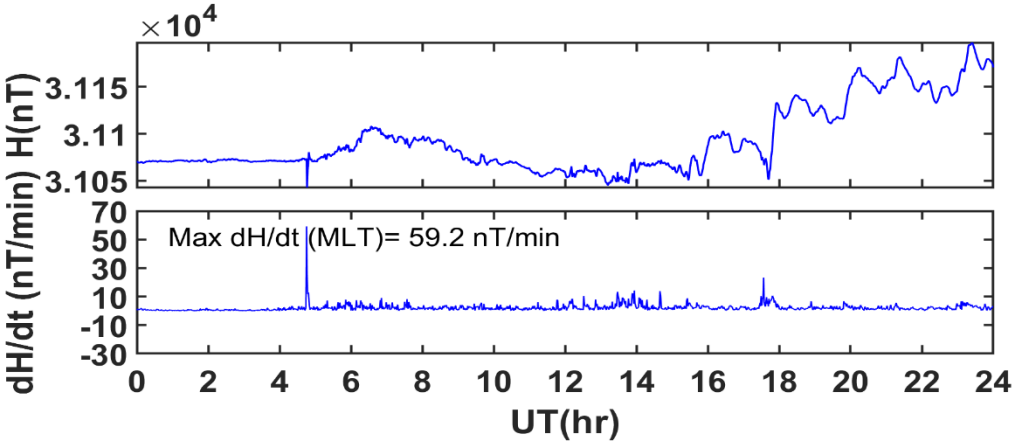

Fig. 21. represents the Measured magnetic field H component and the calculated (dH/dt) values on March 17th, 2015.

Year 2017:

We studied the strongest two storms in 2017. The geomagnetic storm developed over two successive days, 7th and 8th of September 2017.

Data on 7th and 8th of September:

A CME hit the Earth's magnetic field on the first day developing a G3 geomagnetic storm, the storm commenced at 23:00UT as obvious in SYMH and AU, AL indices. On the second day another wave hit the magnetosphere at mid-day (about 12 UT) generating a G4 geomagnetic storm with a maximum Kp index of 8

(figure 22). As a result of both strikes, the geomagnetic field reverberated violently at times of CME arrival at the magnetosphere, showing sharp variations in the magnetic field H-component. However, a maximum value of ($\frac{dH}{dt}$) showed to be 29.9 nT/min at around 23 UT which is 1 LT the following day (figure 23)

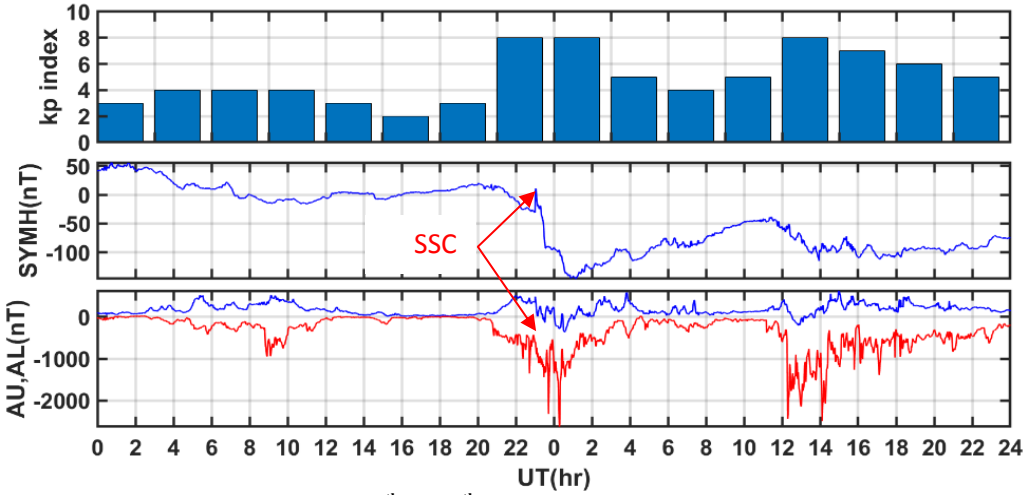

Fig. 22. Geomagnetic activity indices on 7th and 8th of September 2017. The panels from top to bottom, kp index, SYMH index in nT finally, AU (blue) and AL (red) indices in nT.

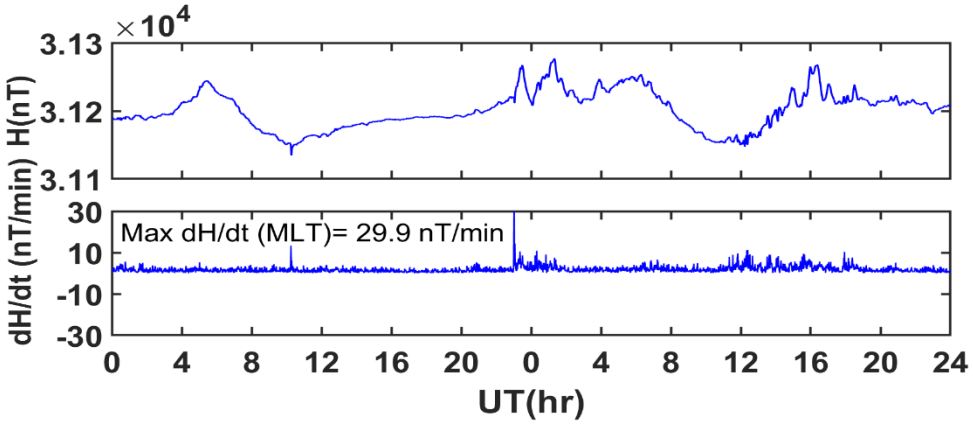

Fig. 23. represents the Measured magnetic field H component and the calculated (dH/dt) values on 7th and 8th of September 2017.

GICs along ACSR conductors:

The amplitude of GIC depends on the geomagnetic source field as well as the power system characteristics. The major system characteristic that controls the amplitude of GIC is the resistance of the system components. So here we estimate the GIC that would flow along the Aluminum Conductor Steel Reinforced (ACSR) using the maximum (dH/dt) value of each studied day and the resistance per unit length for each conductor. We considered the ACSR conductors in our study as they are widely used in the Egyptian power networks.

The following graphs represent the estimated GIC amplitudes generated along the (ACSR) conductors using their resistance values, which are listed in table 3.

Table 3. represents the resistance of different (ACSR) conductors. Link for ACSR pecification https://www.eehc.gov.eg/CMSEehc/media/53slvg1m/edms-04-100-1.pdf

Conductor's Code'	Conductor's Old code	DC Resistance Ω/km
15-ALl/3-STlA	16/2.5	1.8769
24-ALl/4-STlA	25/4	1.2012
34-ALl /6-STl A	35/6	0.8342
48-ALl/8-STlA	50/8	0.5939
70-ALl/ll-STlA	70/12	0.4132
94-ALl/15-STIA	95/15	0.306
122-ALl/20-STIA	120/20	0.2376
149-ALl/24-STIA	150/25	0.194
184-ALl/30-STIA	185/30	0.1571
209-ALl /34-STIA	210/35	0.1381
243-ALl/39-STIA	240/40	0.1188
304-ALl/49-STIA	300/50	0.0949

Year 2013:

Figure 24. a. provides a maximum current amplitude of 4.2×10^{-4} (A.m) at a 0.0949 (Ω/km) resistance, and a minimum current amplitude of 2.1×10^{-5} (A.m) at a conductor resistance of 1.8769 (Ω/km). While figure 24. b. has higher activity; therefore, it shows a maximum current of 3.57×10^{-4} (A.m) at a 0.0949 (Ω/km) resistance and a minimum current value of 1.8×10^{-5} (A.m) at a resistance of 1.8769 (Ω/km).

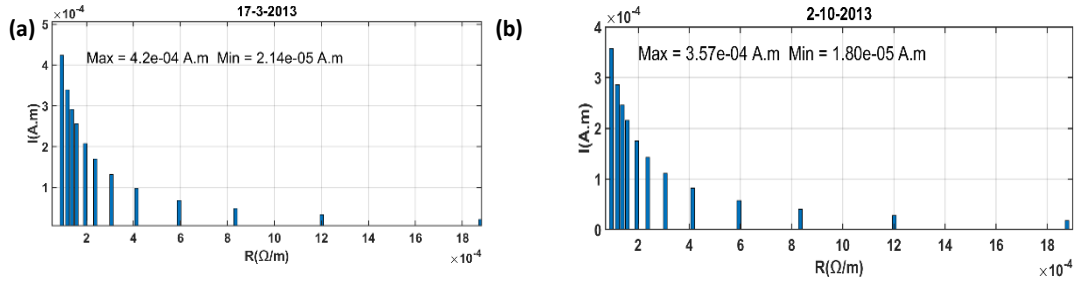

Fig. 24. The estimated induced current along the ACSR conductors versus the resistance of each conductor on (a) March 17th, 2013 and (b) October 2nd, 2013.

Year 2014:

In 2014 we studied 4 geomagnetic storms that differ in activity. Only two storms were chosen, since their Maximum (dH/dt) exceeded 30 nT/min. These two storms are September 12th and December 23rd.

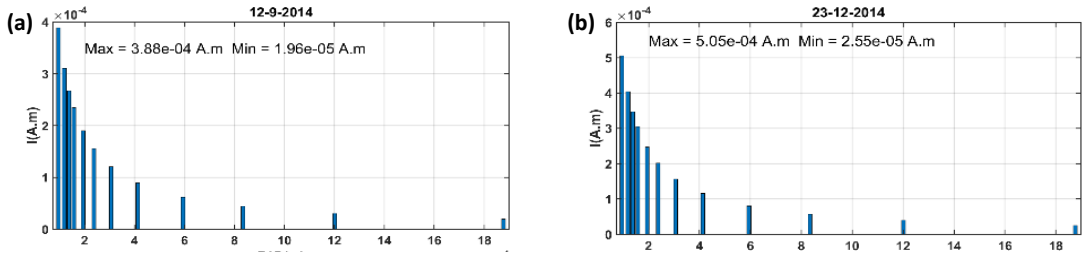

Fig. 25. The estimated induced current along the ACSR conductors versus the resistance of each conductor on (a) September 12th, 2014 and (b) December 23rd, 2014

September 12th was more active than the previous days due to a G3-class GMS, so the maximum estimated current was 3.88×10^{-4} (A.m) along the 0.0949 (Ω/km) conductor and a minimum current of 1.96×10^{-5} (A.m) along the 1.8769 (Ω/km) conductor figure 25. a. December 23rd was the highest activeday of the year, as it has a maximum estimated current of 5.05×10^{-4} (A.m) and a minimum estimated current of 2.55×10^{-5} (A.m) (figure 25.b).

Year 2015:

In 2015, three major storms were studied. One of these storms (March 17th, 2015) was a severe GMS, actually it is considered as the highest active storm in solar cycle 24. Only storms of June 22nd and March 17th are considered, since their Maximum (dH/dt) exceeded 30 nT/min.

A G4-class storm hit on June 22nd causing a maximum current amplitude of 6.26×10^{-4} (A.m) at the 0.0949 (Ω/km) conductor, and a minimum current amplitude of 3.16×10^{-5} (A.m) at a conductor resistance of 1.8769 (Ω/km) (figure 26. a.). March 17th storm had the most serious effects as it maximized the current to 6.24×10^{-4} (A.m) along the 0.0949 (Ω/km) conductor, and 3.15×10^{-5} (A.m) along the 1.8769 (Ω/km) conductor (figure 26. b.), Which are the highest estimated currents along the ACSR conductors this solar cycle.

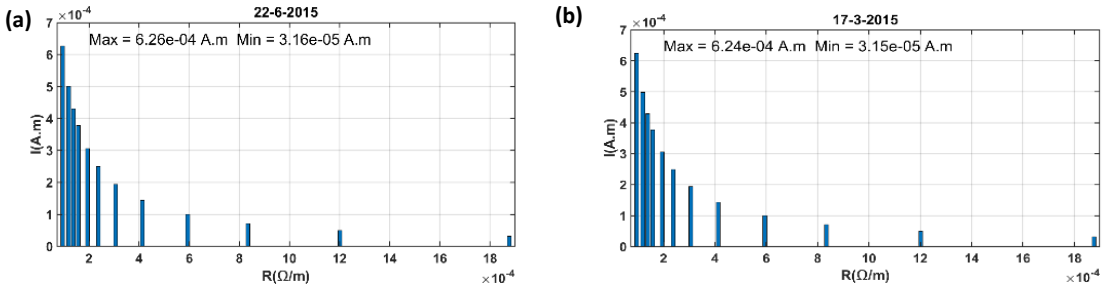

Fig. 26. The estimated induced current along the ACSR conductors versus the resistance of each conductor on (a) June 22nd, 2015, (b) March 17th, 2015.

Year 2017:

During this year we studied the most active storm, which was recorded on September 7th, 2017.

The storm hit the Earth's magnetic field at the end of the first day and continued perturbations to the second day. The maximum estimated current amplitude is 3.15×10^{-4} (A.m), while the minimum estimated currents were 1.59×10^{-5} (A.m) on September 7th (figure 27).

It is obvious that the induced current amplitude decreases with increasing resistance, which is compatible with previous studies showing that high voltage powerlines have lower resistance levels and thus higher GIC levels [16, 18, 19] While, lower voltage powerlines possess higher resistance and therefore lower GIC levels. Individual low voltage powerlines may have smaller GIC values; however, multiple low voltage powerlines may have GIC levels comparable with GIC in higher voltage lines [13]. The maximum and minimum calculated GIC values for each day of the studied days are listed in table 4.

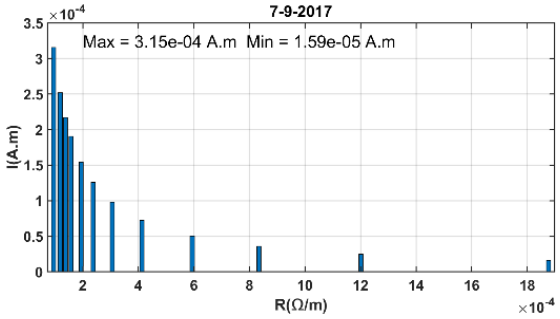

Fig. 27. The estimated induced current along the ACSR conductors versus the resistance of each conductor on September 7th, 2017.

Table 4. represent the maximum and minimum estimated GIC amplitudes along the ACSR conductors on each day of the studied days.

Date	Max. GIC (A.m) (Conductor Resistance 0.0949 (Ω/km))	Min. GIC (A.m) (Conductor Resistance 1.8769 (Ω/km))
17-03-13	4.23×10^{-04}	2.14×10^{-05}
02-10-13	3.57×10^{-04}	1.80×10^{-05}
12-09-14	3.88×10^{-04}	1.97×10^{-05}
23-12-14	5.05×10^{-04}	2.55×10^{-05}
22-06-15	6.259×10^{-04}	3.16×10^{-05}
17-03-15	6.24×10^{-04}	3.15×10^{-05}
07-09-17	3.15×10^{-04}	1.59×10^{-05}

Conclusion

In this study we investigated the rate of change of the magnetic field H component in Egypt and compared our results with [5] own results at the same studied storms upon data availability. ($\frac{dH}{dt}$) values are used as a representative of the induced electromotive force, hence the induced voltage in ACSR conductors during the maximum active days of solar cycle 24 (2012- 2017). We used the Kp index to detect stormy days, with a minimum Kp index of 4. Finally, storms with dH/dt exceeding 30 nT/min were chosen and GICs are estimated along the ACSR conductors using the maximum ($\frac{dH}{dt}$) value for each storm and the conductor's resistance. Our significant conclusions are summed up in the following points.

- Among the four compared stations (MLT, LKW, BCL and PTN) Misallat (MLT) and PTN stations have shown the lowest ($\frac{dH}{dt}$) rates. On the other hand, LKW and BCL have shown the highest ($\frac{dH}{dt}$) rates due to their equatorial location, in which there is direct GIC enhancement due to equatorial electrojet current.
- At the MLT station ($\frac{dH}{dt}$) has exceeded 30 nT/min during six storms. The highest (dH/dt) was recorded on 22nd, June 2015 to be 59.4 nT/min followed by Saint Patrick's storm on 17th, March 2015, with a maximum value of 59.2 nT/min which insures the occurrence of GIC at that day.
- In most of the storms the maximum ($\frac{dH}{dt}$) value coincides with the same time of the storm commencement; however, it does happen that the maximum value of ($\frac{dH}{dt}$) occurs two hours after the storm commencement on October 2nd, 2013, and on July 15th, 2012 the maximum value has detected 15 hours after the CME strike.
- GIC estimations along the ACSR conductors has shown greater values at lower conductor resistance and it decreased with increasing resistance.

- The maximum calculated GIC values along the conductor with the lowest resistance of 0.0949 (Ω/km) spans a range of values from 4.23×10^{-4} (A.m) to 3.15×10^{-4} (A.m).
- The minimum calculated GIC values along the conductor with the highest resistance of 1.8769 (Ω/km) spans a range of values form 1.59×10^{-5} (A.m) to 2.14×10^{-5} (A.m).
- Our GIC results only applies for the ACSR conductors as they are calculated using the conductors' own resistance.
- Based on the research results, Egypt is highly susceptible to GICs during strong geomagnetic storms, so we need to consider GIC occurrence in Egypt.
- We highly recommend precise network planning, also we suggest numerical modeling and testing prior to network foundation.

References

[1] Wik, A., Viljanen, A., Pirjola, R., Pulkkinen, A., Wintoft, P. and Lundstedt, H., *Sp. Weath.*, 6, S07005, (2008).

[2] Zawawi, A.A., Ab Aziz, N.F., Abidin, M.Z., Hashim, H. and Mohammed, Z., Sust, 12, 9225, (2020).

[3] ANSI C57. " An American National Standard IEEE Guide for Transformer Through-Fault-Current Duration ". IEEE, 109 (1985).

[4] Bolduc, L., *J Atmos Sol Terr Phys*, 64, 16, (2002).

[5] Anuar, N.M., Kasran, F.A., Abbas, M., Jusoh, M.H., Ab Rahim, S.A., Abdul Hadi, N.,Yoshikawa, A.and Radzi Z. M., *J. Phys. Conf. Ser.*, 1152, 1, (2019).

[6] Watari, S., Nakamura, S., and Ebihara, Y., Japan. Earth, Planets and Space, 73, 1, (2021).

[7] Tozzi, R., Coco, I., and De Michelis, P., Ann. of Geoph., Roma, Italy, 61, (2018).

[8] Carter, B.A., Yizengaw, E., Pradipta, R., Weygand, J.M., Piersanti, M. and Pulkkinen, A., J. Geophys. Res. Space Physics, 121, 10, (2016).

[9] Espinosa, K.V., Padilha, A.L., and Alves, L.R., *Sp. Weather*, 17, 2, (2019).

[10] Oliveira, D.M., "Arel, D., Raeder, J., Zesta, E., Ngwira, C.M., Carter, B.A., Yizengaw, E., Halford, A.J., Tsurutani, B.T. and Gjerloev, J.W., *Sp. Weather*, 16, 6, (2018).

[11] Belakhovsky, V., Pilipenko, V., Engebretson, M., Sakharov, Y. and Selivanov, V., *J. Sp. Weather Sp. Clim.*, 9, A18, (2019).

[12] Kasran, F.A.M., Jusoh, M.H., Ab Rahim, S.A.E. and Abdullah, N., *ICSET 2018 - 2018 IEEE 8th Int. Conf. Syst. Eng. Technol. Proc.*, October, (2019).

[13] Boteler, D.H. and Pirjola, R.J., *Sp. Weather*, 15, 1, (2017).

[14] Abd Latiff, Z.I., Anuar, N.M., Jusoh, M.H., Ab Rahim, S.A.E., *IEEE 8th Int. Conf. Syst. Eng. Technol.*, October, (*2018).*

[15] Kelbert, A., Surv. in Geophys., Netherlands, 41, 1, (2020).

[16] Torta, J.M., Marsal, S. and Quintana, M., *Earth, Planets Sp.*, 66, 1, (2014).

[17] Thomson, A.W.P., Gaunt, C.T., Cilliers, P., Wild, J.A., Opperman, B., McKinnell, L.-A., Kotze, P., Ngwira, C.M. and Lotz, S.I., *Adv. Sp. Res.*, 45, 9, (2010).

[18] Kappenman, J. G. "The Electric Power Engineering Handbook". , CRC Press/IEEE Press, Boca Raton, Fla., pp. 16-1–16–22 (2007).

[19] Zheng, K., Boteler, D., Pirjola, R.J., Liu, L.-G., Becker, R., Marti, L., Boutilier, S. and Guillon, S.,

IEEE Trans. on Pow. Del. 29, 2, (2014).

https://kp.gfz-potsdam.de/en/

https://wdc.kugi.kyoto-u.ac.jp/wdc/Sec3.html

https://www.eehc.gov.eg/CMSEehc/media/53slvg1m/edms-04-100-1.pdf

Acknowledgement:

We acknowledge the GFZ German Research Centre for Geosciences and World Data Center (WDC) for Geomagnetism, Kyoto for providing the geomagnetic indices (Kp, SYMH and AU&AL) (https://wdc.kugi.kyoto-u.ac.jp/wdc/Sec3.html).

دراسة حالة للتيارات المستحثة جيومغناطيسيًا (GICs) على طول موصل علوي افتراضي من الألومنيوم المقوى بالفولاذ (ACSR) أثناء العواصف الجيومغناطيسية النشطة في مصر

نوران محمد عمر [1]، طارق عرفة حامد [2]، محمد يوسف قندول [1] و أيمن محروس [3]

[1] قسم الفيزياء، كلية العلوم، جامعة حلوان، القاهرة، مصر.

[2] قسم المغناطيسية الأرضية، المعهد القومي لبحوث الفلك والجيوفيزياء(NRIAG) ، القاهرة، مصر.

[3] قسم العلوم الأساسية والتطبيقية، كلية الهندسة، الجامعة المصرية اليابانية للعلوم والتكنولوجيا، الإسكندرية، مصر.

تم اجراء العديد من الدراسات حول العالم عن التيارات المستحثة جيومغناطيسيا (GICs) و معظم هذه الدراسات عند دوائر عرض قطبية و استوائية، و ذلك لإرتفاع شدة التيارات (GICs)هناك، حيث يتم تعزيزها من خلال التيارات الكهربائية الشفقية و التيارات الكهربائية الاستوائية.

و خلال هذه الدراسة التي نحن بصددها نقوم بإجراء تحليلاتنا في منطقة دوائر العرض القريبة من خط الاستواء بالأخص في مصر و ذلك خلال فترات أوج نشاط الدورة الشمسية الرابعة و العشرين. و بإستخدام بيانات المجال المغناطيسي المأخوذة من محطة المسلات الجيومغناطيسية قمنا بدراسة التغيرات التي تحدث في المركبة الافقية (H) للمجال المغناطيسي في تلك المحطة و مقارنتها بمحطات اخري و التي تقع بالقرب من خط الاستواء، معتمدين علي البيانات المتاحة. معظم العواصف التي قمنا بدراستها تتزامن اعلي قيمة لل ($\frac{dH}{dt}$) مع البداية المفاجأة للعاصفة (SSC). بينما تتحقق اعلي قمية لل($\frac{dH}{dt}$) لبعض العواصف اثناء الطور الاساسي (main phase) للعاصفة. و تم تقدير اعلي قيمة لل($\frac{dH}{dt}$) في محطة المسلات خلال فترة الدراسة ب 59.4 نانوتسلا/دقيقة في يوم 22 يونيه 2015 يليها 59.2 نانوتسلا/دقيقة في اثناء عاصفة سانت باتريك.

و ختاما، فقد تم تقدير قيم ال (GICs) المتولدة في موصلات الالومينيوم المعززة بالصلب (ACSR) علي اختلاف قيم المقاومة الخاصة بها لتظهر اعلي قيمة وهي، 423.6 امبير.كم و ذلك في الموصل ذو المقامة 0.0949 اوم/كم، و 21.4 امبير.كم في الموصل ذو المقامة 1.8769 اوم/كم.